DOI: 10.1002/adem.200700214

Performance of Thin-Film Lithium Energy Cells under Uniaxial Pressure**

By *Tony Pereira*,* *Roberto Scaffaro*, *Zhanhu Guo*, *Simon Nieh*, *Jeff Arias* and *H. Thomas Hahn*

Lithium batteries have attracted much interest in recent years due to their superior performance. They consist of a lithium-ion intercalation cathode and a lithium-metal anode separated by a lithium-ion conducting electrolyte. Over the past decades, much effort has been spent to improve the electrodes and electrolytes for better performance in terms of energy storage, robustness and durability.[1,2] One of the most important goals in this direction has been the design of thin-film lithium batteries since the early 1990's.[3–6] However, real interest arose only with the development of the lithium phosphorus oxynitride (LiPON) solid electrolyte.[7–11] These batteries with thicknesses as thin as 10 μm offer an excellent combination of power and energy density. Such unique physical properties allow their usage in multifunctional energy-storage structures which are not only load bearing but also energy storing. Typical examples of multifunctional applications are electrically propelled unmanned aerial vehicles (UAVs) and micro air vehicles (MAVs), in which the integration of the batteries in the structure is crucial for their full realization.[12,13] The advent of thin-film batteries opens the possibility to use local autonomous power in new applications such as micro-electro-mechanical systems (MEMS), tire pressure sensors, and broadband antenna design.[22]

[*] *Dr. T. Pereira, Dr. Z. Guo*
Mechanical and Aerospace Engineering Department
University of California, Los Angeles, CA 90095
E-mail: apereira@ucla.edu
Dr. R. Scaffaro
Dipartimento di Ingegneria Chimica dei Processi e dei Materiali
University of Palermo, Italy
Dr. S. Nieh, Dr. J. Arias
Front Edge Technologies Inc.
Baldwin Park, CA
Prof. H. T. Hahn
Materials Science and Engineering Department
University of California, Los Angeles, CA 90095
E-mail: hahn@seas.ucla.edu

[**] *This work was carried out at the Multifunctional Composites Laboratory (MCL), University of California Los Angeles under the Air Force Office of Scientific Research MURI Grant FA9550-05-1-0138 to University of Washington, managed by Dr. B. Les Lee.*

In view of such applications, and to increase the mechanical reliability of these systems, it is worth knowing the relations between the electrical performance, in particular charge and discharge cycles, and other physical parameters such as temperature, flexural deformation and uniformly distributed pressure over their entire surface area.

The effect of temperature has been widely studied, together with some solutions proposed to increase the thermal stability of the batteries.[14–17] Above a certain temperature, reactions occurring in the electrodes rapidly lead to the failure of the energy cells. A number of studies have been carried out to find out the relations between the electrical behaviour and the temperature[14–16] including the effect of thermal stabilizers[17] and the modelling of the phenomena.[18] The all-solid-state thin-film lithium energy cells used in this study have an upper operating temperature limit of 150 °C claimed by the manufacturer, albeit operation at higher temperatures will result in shorter lifetimes. While the study of the effect of temperature exists, no literature is available to correlate the mechanical loading of uniformly distributed uniaxial pressure with the electrical charge/discharge performance of these energy cells.

The aim of this work series is to find the relations between the electrical performance of all-solid-state thin-film lithium energy cells when subjected to mechanical stresses. In the first part of this work,[19] we analyzed the effect of flexural deformations on the charge/discharge characteristics of these thin-film energy cells. In this present work, the effect of uniformly distributed uniaxial surface pressure on the electrical performance of the energy cells was investigated. The knowledge of the relations between pressure and electrical properties of the energy cell is necessary to fabricate the laminated composites with these devices embedded. The fabrication of laminated composites requires a constant pressure of about 550 kPa in an autoclave with curing times of one to several hours. Although flexural bending tests and pressure tests are similar in terms of their mechanical nature, they do not give the same response in the energy cells because of the different solicitations on the several components of the energy cell. Hence, it is required to study these solicitations individually and separately.

Experimental Procedure

All energy cells in this study were provided by Front Edge Technologies (Baldwin Park, CA), with square dimensions of about 25 mm on the side and average mass of (0.175 ± 0.025)

COMMUNICATIONS

g from a sample pool of 10 specimens. These energy cells are currently in commercial production, and have a nominal voltage of 3.6 VDC (20). The all solid state thin-film lithium energy cells have a lifetime of 1,000 charge/discharge cycles of up to 100 % depth-of-discharge, and a specific energy of about 200 Wh/kg without considering the packaging mass. In its present configuration, accounting for the packaging mass, yields a capacity of about 2 mAh/g, corresponding to an energy density of about 7.2 Wh/kg. The packaging for the configuration used in this study consists of two equal top and bottom mica substrates of about 50 μm thickness each. The mica used is muscovite, a phyllosilicate mineral of aluminium and potassium with chemical formula $KAl_2(AlSi_3O_{10})(F,OH)_2$ having a highly perfect basal cleavage that yields remarkably thin laminae, often highly elastic. The mica substrates are held together all around by a 40 μm polymer layer of Surlyn (Dupont) sealant (see Fig. 5). While Surlyn is permeable to ambient oxygen and water vapor, its permeability is very low. The Surlyn low permeability and the energy cell high aspect ratio (cross section thickness vs. length of the sealant) at the edges justifiy its use as a sealant in thin-film Li batteries. This sealing strategy gives a maximum 2-year battery lifetime. The geometric profile of specimen 0606015 is shown in Figure 1. Circles refer to the thickness in the area of active components of the energy cell, i.e., anode, cathode, electrolyte and the mica substrates. Boxes refer to the thickness at the edge all around the energy cell where there are no active components, i.e., only the mica substrate and the sealant exist.

Two energy cells were initially subjected to three initial consecutive charge/discharge cycles under no uniaxial pressure to establish a performance baseline for reference and comparison. The charging was done at a constant voltage of 4.2 VDC and a limiting current draw of 1 mA using a Keithley SourceMeter 2400 under GPIB control of a MDS C program written specifically for this purpose. The data acquisition and analysis flowchart is shown in Figure 2. The real time discrete current and voltage were measured at one-second intervals and logged to a text data file with cycle start/end times and time sequence for each data set. Each specimen was considered to be fully charged when the charge current fell below 50 μA. Each charge cycle was immediately followed by a discharge at 1 mA constant sink current. The device was considered to be fully discharged when the voltage dropped to a value of 3.0 VDC. The energy cell was held flat, that is, without flexural deformations, for the entire set of tests done in this study. The charge/discharge current of 1 mA used in this work corresponds to an average 2.5 C discharge ratio (1 mA/0.4 mAh), which is more severe than the commonly used nominal discharge ratio of 1 C found in the literature.[23] However, the former value is within the normal operating parameters for this type of batteries, which can accept charge/discharge ratios higher than what are normally expected without suffering damage.

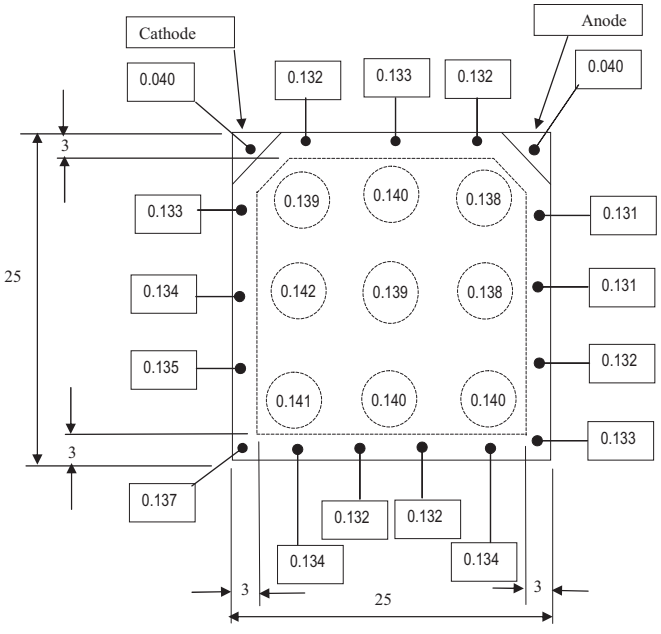

Fig. 1. Geometry and thickness profile (dimensions in mm). Circles refer to the thickness in the area of active components of the energy cell. Boxes refer to the thickness at the edge all around the energy cell.

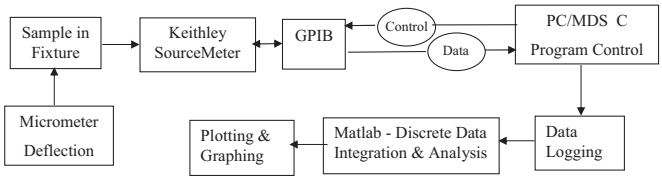

Fig. 2. Data acquisition and control flow diagram.

The discharge is used to define the energy cell capacity C in units of mAh. The discrete data acquired was taken to Matlab and integrated using the trapezoidal method to calculate the energy cell capacity, with the total charge/discharge adjusted for time accuracy. The energy cell capacity is defined as follows:

$$C = \int_0^{\tau} i dt \tag{1}$$

where τ is the upper limit of integration corresponding to the time during charge at which the current $i(t)$ = 50 μA is reached, or the time at which during discharge the voltage $v(t)$ = 3.0 VDC is reached. The first three consecutive charge/discharge cycles under no physical solicitations were used to establish the characteristic baseline behaviour of each energy cell.

A fixture was designed and fabricated by the author using an insulating machinable wax of appropriate strength on a micro-machining centre. Machining tolerances for the fixture were kept at very low levels, to within less than about 50 microns, measured with Mitutoyo digital calipers. The schematic diagram of the fixture is shown in Figure 3, with the actual pictures in Figures 4(a), 4(b) and 4(c). A cavity was

ADVANCED ENGINEERING MATERIALS

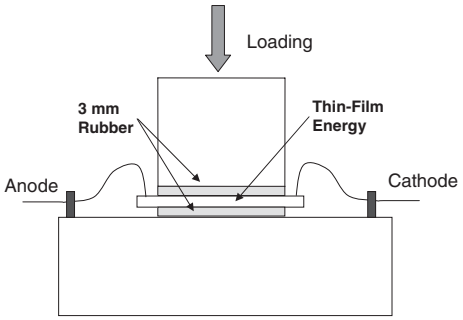

Fig. 3. Schematic of pressure test fixture.

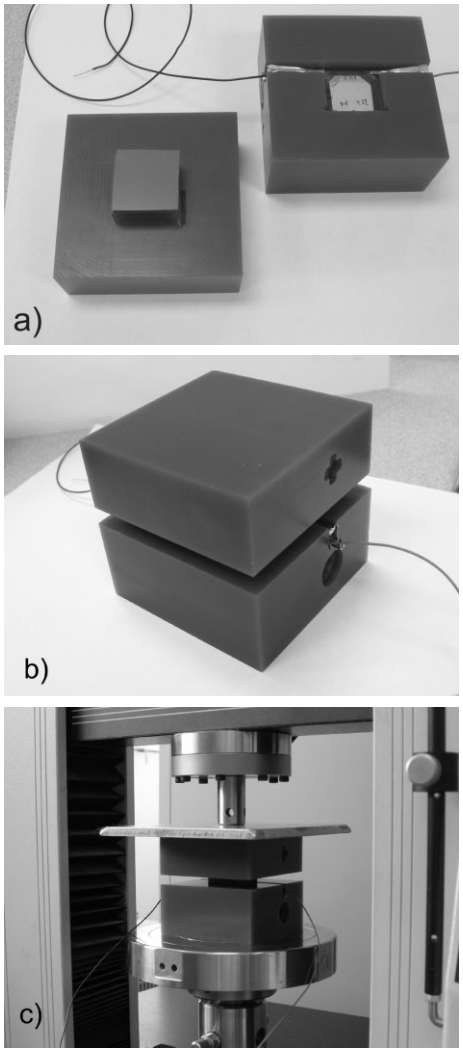

Fig. 4. Rapid Prototype pressure test fixture; a) Open, showing electrical contacts and rubber cushioning; b) Closed, assembled; c) Installed on a mechanical testing machine.

formed to accommodate the energy cell specimen, with channel conduits for the electrode terminal connections, and sufficient height to cushion both the top and bottom sides of the energy cell with about 3 mm of a soft rubber material. Electrical contacts to the energy cell were established by using a conductive rubber (Zoflex, CD45.1-6S-2) with flat alligator clips, and the electrical signals were taken to the Source-Meter. The conductive rubber pad between the energy cell electrode and the alligator clips may contribute to some energy dissipation. However, due to the very low thin-film thickness of the energy cell electrodes (100 nm) and the dynamic character of the experiment, the rubber foam contact was found to be both more durable and reliable.

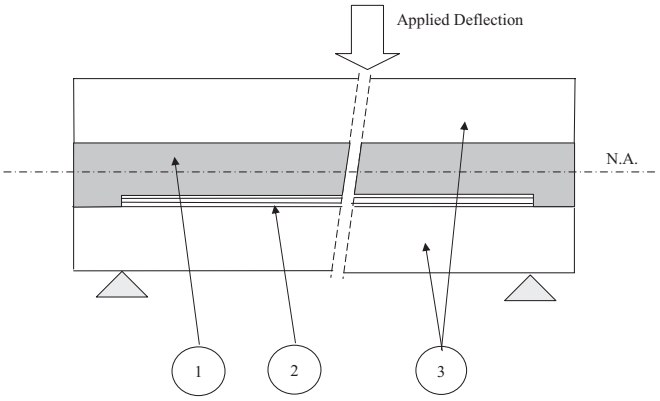

Fig. 5. Cross-sectional schematic of energy cell. Scale is approximate. 1. Sealant 40 μm (mica substrate bends slightly at the edge); 2. Active Component Layer: anode (Li-metal 2 μm thick, LiPON electrolyte 2 μm thick, lithium cobalt oxide cathode 6 μm thick, respectively); 3. Mica substrate 50 μm thick.

A tensile test was performed on another separate energy cell to determine its mechanical properties. The Young's Modulus was found to be 107 GPa, and the failure strength was found to be 80 MPa. The measured tensile properties of the energy cell are attributed mostly to the mica (muscovite) substrate.[19] The cross-sectional profile reveals that the active components (anode, electrolyte and cathode) are very thin, ~ 10 μm, relative to the total thickness of the two mica substrates, ~ 100 μm, Figure 5.

Results and Discussion

Typical profiles of charge and discharge capacities measured on the first energy cell during the first three baseline cycles are shown in Figure 6. The average capacities measured for two energy cells are (0.3595 ± 0.0039) mAh and (0.3815 ± 0.0048) mAh respectively, based on a total of 3 measurements per charge or discharge, respectively. The small difference observed between the charge and discharge capacities indicates that only a small amount of energy loss or hysteresis occurred. This energy dissipation is due to electrochemical losses inside the energy cell involving internal resistance and chemical changes, and it is transformed into heat and other losses.

The results of the pressure cycle experiments from the first specimen are shown in Figure 7. The all-solid-state thin-film lithium energy cell was charged and discharged under constant uniaxial pressure at each incremental pressure step, while holding that pressure uniformly constant throughout the entire charge/discharge cycle. The data is plotted twice in different forms for clarity, both bar and line form. While the bar graph is better at depicting the contrast between the

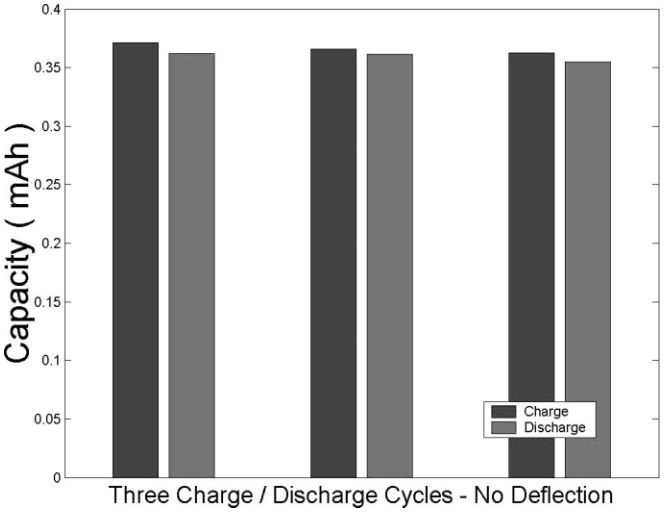

Fig. 6. Baseline for three charge/discharge capacities with no pressure for specimen 06030006 (left bar is charge, right bar is discharge). Average charge: (0.3665 ± 0.0044) mAh; average discharge: (0.3595 ± 0.0039) mAh.

charge/discharge capacities, the line graph shows the hysteresis in the charge/discharge cycles more clearly.

The results of the uniaxial pressure charge/discharge cycle experiments in Figure 7 indicate that the capacity of this specimen decayed from the baseline level established at zero pressure to a fairly stable plateau with a mild slope. Up until a uniaxial pressure of about 0.8 MPa was reached, the charge/discharge capacities within this plateau are well within the data deviation regardless of the amount of pressure applied. After a uniaxial pressure of 0.83 MPa was reached, capacities started to drop noticeably until failure occurred at 2.8 MPa, when it failed to charge. Visual observation revealed that the top mica substrate of the energy cell was separated from the Surlyn sealant and peeled off, exposing the underlying layer of lithium-metal to the ambient air, thus leading to its rapid oxidation. The charge failure can be explained by the structural failure of the sealant. This structural failure occurred suddenly above a certain pressure, which indicates that the sealant layer was squeezed out between the lithium layer and the mica substrate once the pressure was sufficiently high for the sealant to fail. Any broken seal allowing air into the device will cause rapid deterioration of the active layers leading to charge failure.[21] The lithium-metal anode of this energy cell with a uniform shiny silvery color turned almost completely black within seconds, as a result of oxidation (Fig. 8(a), 8(b)) from contact with ambient air, and the energy cell did not take any further charges. The compressive strength of Lipon is typically several hundred MPa. The pressures used in this study are well below the critical pressure of Lipon and will not affect the charge/discharge performance of the energy cell. Under very high pressures, the failure of the battery could be caused by cracks in the Lipon microstruture. However, the stresses in this study remained relatively low. Other parts of the battery such as the Surlyn sealant that squeezed out of the energy cell edges proved to be structurally more critical than the Lipon itself.

Another energy cell (06060015) was tested to confirm the test results discussed heretofore. Typical charge and discharge capacities measured under no mechanical solicitations for the second energy cell during the first three baseline cycles are shown in Figure 9. The average charge and discharge capacities measured were (0.3930 ± 0.0011) mAh and (0.3815 ± 0.0048) mAh, respectively, based on a total of 3 measurements per charge or discharge, respectively.

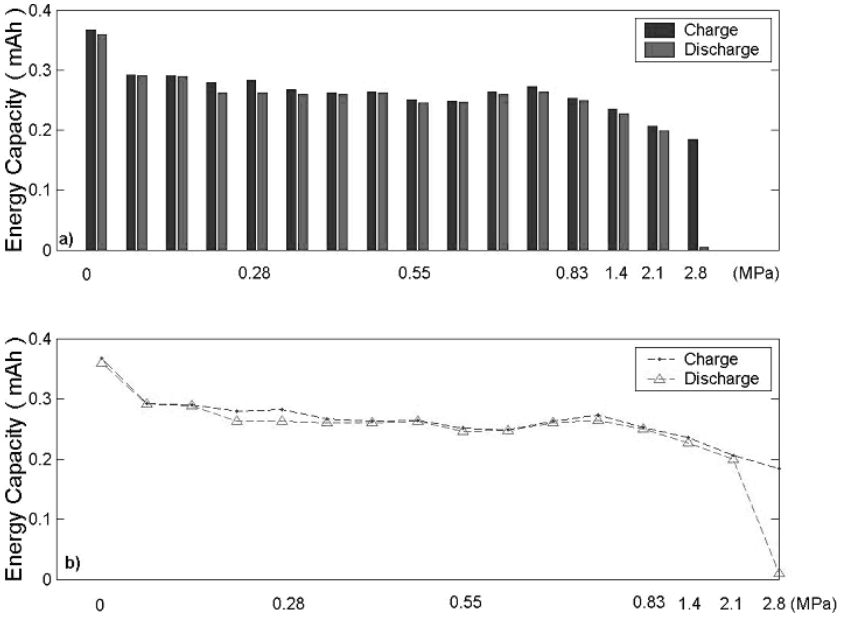

Fig. 7. Charge/discharge capacity results for sample 06030006: a) Charge (left bar) and discharge (right bar) at each pressure increment; b) Plotted in line mode to illustrate hysteresis. Average charge: 0.2635 ± 0.0398 mAh; average discharge: 0.2467 ± 0.0715 mAh.

Figures 10 (a) and (b) show the charge and discharge cycles with an incremental uniaxial pressure increase of 70 kPa for the second energy cell. Up to about 1.5 MPa of uniaxial pressure, the charge/discharge capacities are within the data scatter, and there was no visible sign of energy cell degradation. Above 1.5 MPa uniaxial pressure, there is a slight decay in energy cell capacity up to 2.0 MPA. Above the latter pressure, the decay is more pronounced and energy cell failure occurs eventually at 2.3 MPa pressure. A similar, sudden failure above a high pressure was also observed, indicating that the sealant layer was squeezed out between the lithium layer and the mica substrate. Figure 10(b) shows the same data as Figure 10(a) plotted in line mode to illustrate hysteresis more clearly.

Figure 11(a) shows the charge cycle for one energy cell under the first uniaxial pres-

ADVANCED ENGINEERING MATERIALS

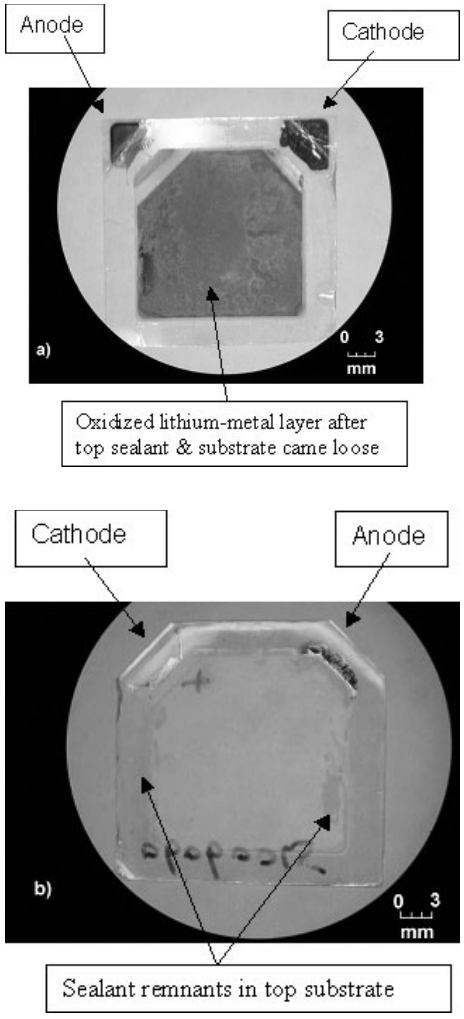

Fig. 8. Substrate separation due to sealant structural failure for sample 06030006: a) Bottom substrate with thin-film deposition layers on top, showing lithium-metal oxidized topmost layer b) Top substrate seen from the bottom side that was in contact with the lithium-metal top layer shown in a). Remnants of the sealant layer can be clearly seen.

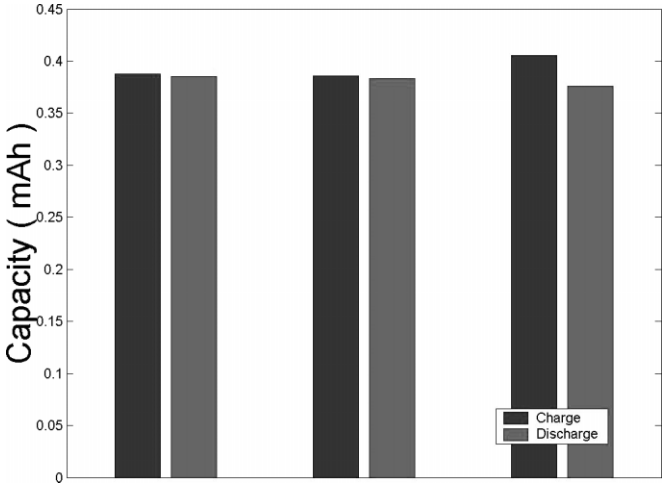

Fig. 9. Baseline for three charge/discharge capacities with no deflection for specimen 06060015 (left bar is charge, right bar is discharge). Average charge: 0.3930 ± 0.011 mAh; average discharge: 0.3815 ± 0.0048 mAh.

sure increment to about 70 kPa immediately after the baseline testing. As soon as a constant charge of 1 mA starts at time zero and at 4.2 VDC, the energy cell voltage reads 3.904 VDC and then slowly rises to the charge voltage in about 700 s. The current then starts to drop quickly, and the specimen was considered fully charged when it reached 50 μA in about 1,200 s. The resulting capacity of the device was calculated to be 0.3783 mAh. Figure 11(b) shows the discharge immediately following the preceding charge at the same pressure, with an initial voltage of 4.190 VDC, which is slightly lower than the charge voltage. At a constant discharge current of 1 mA, the voltage drops at a fairly constant rate below 4 VDC. When it reaches about 3.8 VDC in 1,200 s, the voltage quickly drops to 3.0 VDC, and the specimen is considered to be fully discharged. The resulting discharge capacity was calculated to be 0.3722 mAh. Figures 11(c) and (d) show a very similar charge and discharge behavior for the same specimen when loaded to about 1 MPa uniaxial pressure. The resulting charge capacity was 0.3769 mAh and the discharge capacity was 0.3722 mAh, respectively. Figures 11 (e) and (f) show the charge/discharge pattern for the same energy cell when loaded to about 2.2 MPa. At this ending pressure, the charge time was longer than the 1,200 s shown in the preceding diagrams, which resulted in a charge capacity of 0.3182 mAh lower than that of the 0.3930 mAh charge baseline. Also at the same uniaxial pressure, the shorter discharge time of about 1,000 s resulted in a discharge capacity of 0.3038 mAh, which is also lower than that of the 0.3815 mAh earlier obtained discharge baseline. Both charge and discharge values are substantially outside the data scatter range. The failure occurred in a mechanism similar to that shown in Figures 8 (a) and (b).

Conclusions

The objective of this study was two-fold. The first objective was to determine if the all-solid-state thin-film lithium energy cells could withstand the minimal 550 kPa uniaxial pressure required for composite manufacturing, which both specimens successfully did. The second objective was to determine the upper boundary uniaxial pressure limit of operation for the all-solid-state thin-film lithium energy cells. The two all-solid-state thin-film lithium energy cells tested in the present study under uniaxial pressure performed well even when subjected to uniaxial pressures up to about 2.0 MPa. However, pressures higher than this value led to their degradation. The observed degradation was due to the mechanical failure of the sealant. Above this pressure, the sealant was squeezed out of the space between the two mica substrates and the lithium-metal anode layer, which in turn allowed the ambient air to penetrate into the energy cell core, thus leading to the rapid degradation of the charge and discharge performance and the ultimate demise of the energy cell. We found out that, within the observed range, uniformly distributed

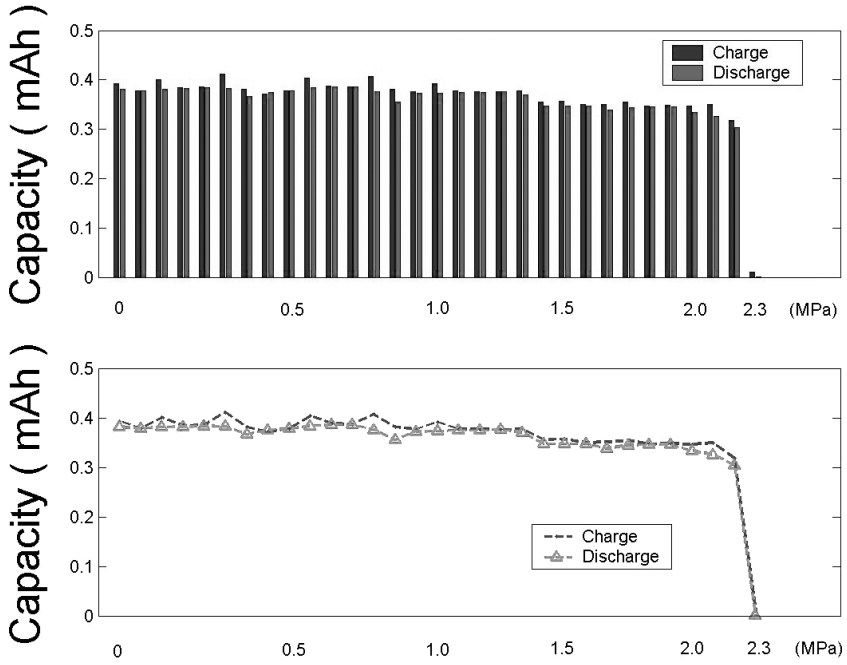

Fig. 10. Charge/discharge capacity results for sample 06060015, from 0-2.23 MPa pressures: a) Charge (left bar) and discharge (right bar) at each pressure increment; b) Plotted in line mode to illustrate hysteresis. Average charge 0.3618 ± 0.0686 mAh; average discharge: 0.3521 ± 0.0684 mAh.

uniaxial pressure had little or no effect on the charge/discharge performance of the all-solid-state thin-film lithium energy cells. Other power charge/draws outside of 1 mAh were not of interest in this study for the reasons already pointed out, albeit that they may be considered for future studies. Apart from other considerations for failure due to the current packaging characteristics, we found that all-solid-state thin-film energy cells charge/discharge cycles under upwardly increasing uniform uniaxial pressure are extraordinarily robust and resilient to the effects of uniaxial, uniformly distributed pressure and constant power charge/sink of 1mAh. If the overall structure of the energy cell is mechanically robust, i.e., of high structural integrity, the maximum pressure that can be imposed is expected to be much higher than the maximum values noted earlier.

The present study indicates that all-solid-state thin-film energy cells can be used as an integral part of a load-bearing multifunctional, smart material structure if their packaging is of sufficiently high structural integrity. Hence, the goal of using fiber reinforced laminated composites as the packaging material for all-solid-state thin-film batteries in multifunctional smart materials structures is well within reach.

Received: August 25, 2007
Final version: December 03, 2007

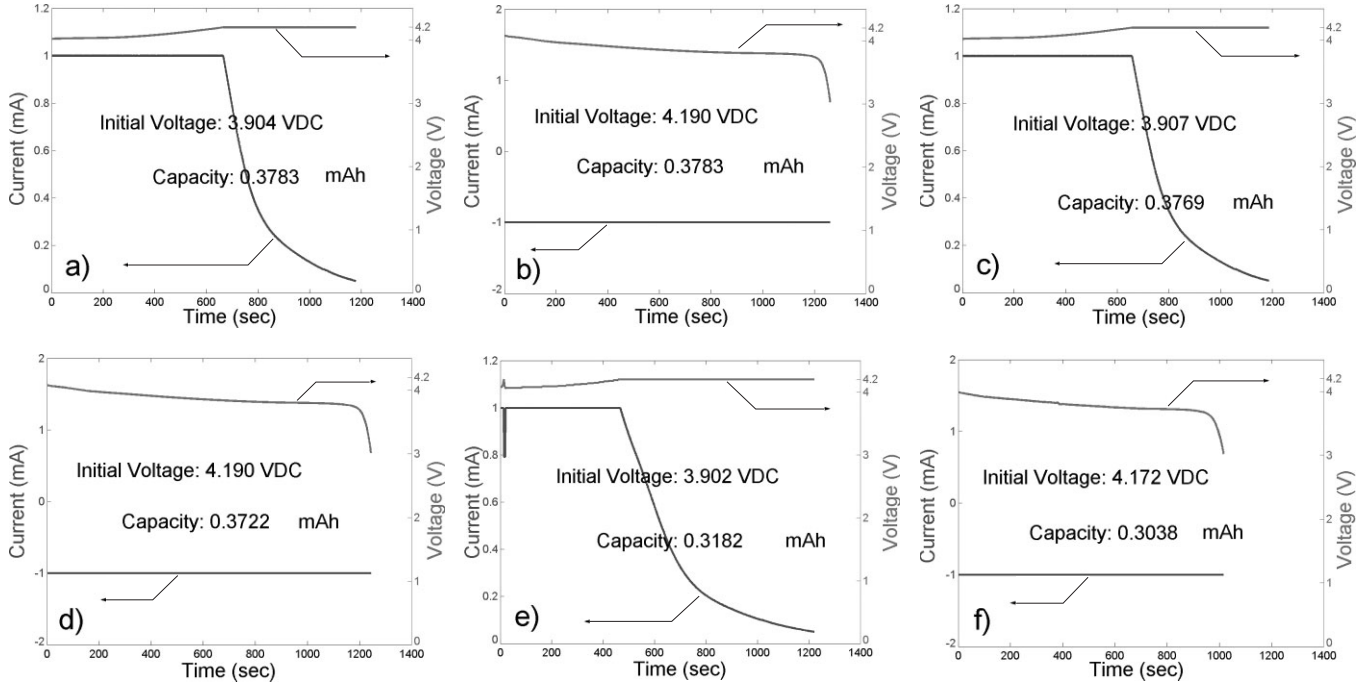

Fig. 11. Charge/discharge behaviour for specimen 06060015: a) First charge starts at 70 kPa pressure; b) followed by discharge at the same pressure; c) charge at 1.0 MPa pressure; d) discharge at the same pressure; e) charge ending at 2.2 MPa pressure; f) discharge ending at the same pressure.

[1] A. S. Aricò. P. Bruce, B. Scrosati, J. M. Tarascon, W. van Schlkwijk, *Nat. Mater.* **2005**, *4*, 366.
[2] W. Wakihara, O. Yamamoto *Lithium Ion Batteries – Fundamentals and Performance*, Kodansha-Wiley-VCH, Weinhein **1998**.
[3] X. Yu, J. B. Bates, G. E. Jellison, F. X. Hart, *J. Electrochem. Soc.* **1997**, *144*, 524.
[4] S. D. Jones, J. R. Akridge, *J. Power Sources* **1995**, *54*, 63.
[5] S. D. Jones, J. R. Akridge, *Solid State Ionics* **1996**, *86/88*, 1291.
[6] S. J. Lee, H. K. Baik, S. M. Lee, *Electrochem. Commun.* **2003**, *5*, 32.
[7] J. B. Bates, N. J. Dudney, G. R. Gruzalski, R. A. Zuhr, A. Choudhury, C. F. Luck, *J. Power Sources* **1993**, *43–44*, 103.
[8] J. B. Bates, N. J. Dudney, D. C. Lubben, G. R. Gruzalski, B. S. Kwak, X. Yu, R. A. Zuhr, *J. Power Sources* **1995**, *54*, 58.
[9] B. J. Neudecker, N. J. Dudney, J. B. Bates, *J. Electrochem. Soc.* **2000**, *147*, 517.
[10] J. B. Bates, N. J. Dudney, B. J. Neudecker, B. Wang, *New Trends in Electrochem. Technol: Energy Storage Syst. in Electron.* Gordon and Breach, **2000**.
[11] J. Schwenzel, V. Thangadurai, W. Weppner, *J. Power Sources* **2006**, *154*, 232.
[12] J. P. Thomas, M. A. Qidwai, *Acta Mater.* **2004**, *52*, 2155.
[13] M. A. Qidwai, J. P. Thomas, P. Matic, *Proc. SPIE* **2002**, *4698*, 180.
[14] G. Nagasubramanian, D. H. Doughty, *J. Power Sources* **2004**, *136*, 395.
[15] E. P. Roth, D. H. Doughty, *J. Power Sources* **2004**, *128*, 308.
[16] E. V. Thomas, H. L. Case, D. G. Doughty, R. G. Jungst, G. Nagasubramanian. E. P. Roth, *J. Power Sources* **2003**, *124*, 254.
[17] D. H. Doughty, E. P. Roth, C. C. Crafts, G. Nagasubramanian, G. Henriksen, K. Amine, *J. Power Sources* **2005**, *146*, 116.
[18] D. H. Doughty, P. C. Butler, R. G. Jungst, E. P. Roth, *J. Power Sources* **2002**, *110*, 357.
[19] T. Pereira, R. Scaffaro, S. Nieh, J. Arias, Z. Guo, H. T. Hahn. *J. Micromech. Microeng.* **2006**, **16**, 2714.
[20] V. Krasnov, K.-W. Nieh, S.-J. Ting. *Thin Film Battery and Meth. of Manufact.* U.S. Patent No. 6,632, 563, http://www.uspto.gov/.
[21] W. C. West, J. F. Whitacre, V. WHite, B. V. Ratnakumar, *J. Micromech. Microeng.* **2002**, *12*, 58.
[22] J. W. Long, B. Dunn, D. R. Rolison, H. S. White, *Chem. Rev.* **2004**, *104*, 4463.
[23] F. Croce, F. S. Fiory, L. Persi, B. Scrosati, *Electrochem. Solid-State Lett.* **2001**, *4 (8)*, A121.

